

Evaluating automobile's vibration in frequency domain

Yujie Jia^{1,2}, Vanliem Nguyen^{1,2,*}

¹ School of Mechanical and Electrical Engineering, Hubei Polytechnic University, Huangshi 435003, China

² Hubei Key Laboratory of Intelligent Convey Technology and Device, Hubei Polytechnic University, Huangshi 435003, China

* Corresponding author: Vanliem Nguyen, xuanliem712@gmail.com

CITATION

Jia Y, Nguyen V. Evaluating automobile's vibration in frequency domain. *Mechanical Engineering Advances*. 2024; 2(1): 1239. <https://doi.org/10.59400/mea.v2i1.1239>

ARTICLE INFO

Received: 23 October 2023

Accepted: 1 December 2023

Available online: 15 December 2023

COPYRIGHT



Copyright © 2023 by author(s).
Mechanical Engineering Advances is published by Academic Publishing Pte. Ltd. This article is licensed under the Creative Commons Attribution License (CC BY 4.0).
<https://creativecommons.org/licenses/by/4.0/>

Abstract: Excitation of the low frequency not only influences the driver's health but also strongly affects the durability of the automobile's structures. To research the automobile's vibration in the low-frequency region, a dynamic model of the automobile is established to calculate the vibration equations of the automobile in the time region. Based on the theory of the Laplace transfer function, the automobile's vibration equations in the time region are transformed and converted to the automobile's vibration equations in the frequency region. Then, the effect of the automobile's design parameters and operation parameters on the characteristic of the automobile's acceleration-frequency is simulated and analyzed to evaluate the automobile's comfort as well as the durability of the automobile's structures in the frequency region. The research results show that the design parameters of stiffness, mass, and road wavelength remarkably affect the characteristic of the automobile's acceleration frequency. To reduce the resonant amplitude of the acceleration frequency in the vertical and pitching directions of the automobile, the stiffness parameters of the automobiles and tires should be reduced while the mass of the automobile's body should be increased. Additionally, the road's roughness also needs to be decreased, or the road's quality needs to be enhanced to reduce the resonant amplitude of the automobile's acceleration frequency.

Keywords: automobile's dynamic model; complex domain; ride comfort; frequency region

1. Introduction

The isolation systems of the automobile have been used to reduce the vibration excitations from the road surface transmitted to the automobile's body. In the design process of the vehicle's suspension systems, the structures of the suspension system were designed by the spring and damper with the stiffness parameter and damping parameter. The study showed that these parameters greatly affected the ride comfort of the vehicle [1]. In order to enhance the ride comfort of the vehicle or automobile, these design parameters were optimized by the genetic algorithm [2,3]. By searching for the best stiffness and damping parameters for the automobile's suspension systems, the automobile's ride comfort has been then improved in comparison with the passive suspension systems. However, the automobile's ride comfort was still low under the high speeds of the automobile's moving or the automobile's moving on the poor road surface roughness. Therefore, the automobile's suspension systems were improved by using the control damping forces of semi-active suspension systems [4,5] or semi-active air suspension systems [6]. The research results showed that with the control damping forces of the semi-active suspension systems used, the automobile's ride comfort was better than that of the automobile's optimal suspension systems under different operation conditions. However, the research also indicated that the control performance of the semi-active suspension systems strongly depended on the control

method and control rule of the algorithm programs [7,8]. To enhance the control performance, advanced control methods using the Adaboost algorithm and machine learning were applied [9,10]. In the above studies, the dynamic model was established to calculate the vibration equations of the automobile. Then, these vibration equations were built and simulated to compute the automobile's acceleration responses in the time region. The root mean square values of these acceleration responses were then computed to assess the automobile's ride comfort based on ISO 2631-1:1997 [11].

However, ISO 2631-1 showed that the ride comfort and health of the driver were also strongly affected by the vehicle's vibration excitations in the frequency region [11], especially at the excitations in the low frequency from 0.5 to 10 Hz of the road surface when the vehicle is moving. From the random excitations of the road surface built based on ISO 8068 [12], the interaction models of the vehicle and random road surface were established and studied the vibration of the vehicle or cab in the low frequency region [13,14]. Besides, the effect of the design parameters of the isolation systems on the vehicle's vibrations at low frequencies was also evaluated [15,16]. The results indicated that the density of resonant frequencies and resonant amplitudes of the automobile's acceleration-frequency response appeared very much in the low-frequency region, especially at excitations from 0.5 to 4.0 Hz. This not only affected the driver's health but also strongly affected the durability of the automobile's structures and road surfaces. Thus, the resonant frequencies and resonant amplitudes in the automobile's acceleration-frequency response in this excitation range needed to be minimized. These resonant frequencies and resonant amplitudes were directly impacted by the design parameters and operation parameters of the automobiles, such as the stiffness, mass, speed, road surface, etc. Therefore, the effect of the design parameters and operation parameters of the automobiles on the driver's health and the durability of the automobile's structures under different frequency excitations need to be researched and analyzed. However, this issue has not been considered in the existing research.

In the study of free vibrations of beam structures or doubly curved shell panels, the finite element method is applied to calculate the free vibrations of the models [17–20]. The finite element method easily determines the natural vibration frequencies of the structure to calculate the detailed durability. This method can also be applied to research the vibration of the automobile. However, the disadvantage of this method is that it is difficult to evaluate the influence of the automobile's dynamic parameters during movement. Therefore, to research the effect of the design parameters and operation parameters of the automobiles on the driver's health and the durability of the automobile's structures under different frequency excitations of the road surface, a dynamic model of the automobile is established to calculate its vibration equations in the time region. Based on the theory of the Laplace transfer function [21], the automobile's vibration equations in the time region are transformed and converted to the automobile's vibration equations in the frequency region. Then, the effect of the automobile's design parameters and operation parameters on the characteristic of the automobile's acceleration-frequency is simulated and analyzed to evaluate the automobile's ride comfort as well as the durability of the automobile's structures in the frequency region. Enhancing the working performance of the automobile is the goal of this study.

The practical significance of this research is that from the automobile dynamics model, the theory of the Laplace transfer function is applied to study the low-frequency vibrations of the automobile. The influence of automobile design parameters is evaluated in the low-frequency region. From the research results, the automobile's resonant frequencies are determined. This is the basis for determining initial parameters during the vehicle design process to reduce the resonance amplitude in the low-frequency region of the automobile. This can improve the ride comfort and structural strength of the automobile suspension system.

2. Automobile's mathematical model

2.1. Calculating the vibration equations of the automobile in the time region

In order to compute an automobile's vibration equations based on its actual structure, a 2-D automobile dynamics model is established and shown in **Figure 1**. Where four degrees of freedom of the automobile, including the automobile body's vertical vibration, automobile's pitch vibration, front axle's vibration, and rear axle's vibration, are defined by $z, j, z_1,$ and $z_2,$ respectively. The mass of the automobile's body, front axle, and rear axle are also defined by $m, m_1,$ and $m_2,$ respectively. The stiffness and damping parameters of the front and rear axles are also defined by $\{c_1$ and $k_1\}$ and $\{c_2$ and $k_2\}$. The stiffness and damping parameters of front and rear tires are also defined by $\{c_{t1}$ and $k_{t1}\}$ and $\{c_{t2}$ and $k_{t2}\}$. $l_{1,2}$ and $q_{1,2}$ are the distances and vibration excitations of the automobile and tires.

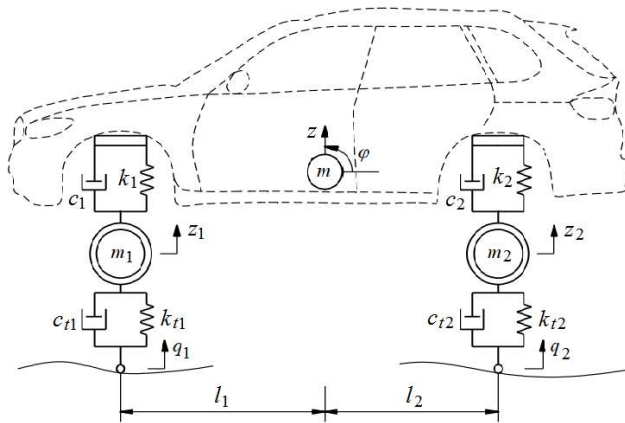


Figure 1. The dynamic model of the automobile.

The four degrees of freedom of the automobile, including the automobile body's vertical vibration, the automobile's pitch vibration, the front axle's vibration, and the rear axle's vibration, are defined by $z, j, z_1,$ and $z_2,$ respectively. The mass of the automobile's body, front axle, and rear axle are also defined by $m, m_1,$ and $m_2,$ respectively. The stiffness and damping parameters of the front and rear axles are also defined by $\{c_1$ and $k_1\}$ and $\{c_2$ and $k_2\}$. The stiffness and damping parameters of front and rear tires are also defined by $\{c_{t1}$ and $k_{t1}\}$ and $\{c_{t2}$ and $k_{t2}\}$. $l_{1,2}$ and $q_{1,2}$ are the distances and vibration excitations of the automobile and tires.

To facilitate the establishment of the vibration equations of the automobile, some

assumptions are made as follows: (1) The deformation of the automobile floor is very small; it is considered absolutely rigid. (2) Under vertical vibration excitation from the road surface when the automobile moves, the horizontal vibration of the automobile body is very small and is ignored. (3) The friction force of the automobile suspension and tires is very small, and it is calculated in the resistance force of the automobile suspension and wheels.

Therefore, from the automobile's dynamics model shown in **Figure 1**, its vibration equations are then written by:

$$\begin{cases} m\ddot{z} + (c_1 + c_2)\dot{z} + (k_1 + k_2)z + (c_1l_1 + c_2l_2)\dot{\phi} + (k_1l_1 + k_2l_2)\phi - c_1\dot{z}_1 - k_1z_1 - c_2\dot{z}_2 - k_2z_2 = 0 \\ I\ddot{\phi} + (c_1l_1^2 + c_2l_2^2)\dot{\phi} + (k_1l_1^2 + k_2l_2^2)\phi + (c_1l_1 - c_2l_2)\dot{z} + (k_1l_1 - k_2l_2)z - c_1l_1\dot{z}_1 - c_1l_1z_1 + \\ + c_2l_2\dot{z}_2 + c_2l_2z_2 \\ m_1\ddot{z}_1 + (c_1 + c_{t1})\dot{z}_1 + (k_1 + k_{t1})z_1 - c_1\dot{z} - k_1z - c_1l_1\dot{\phi} - k_1l_1\phi = c_{t1}\dot{q}_1 + k_{t1}q_1 \\ m_2\ddot{z}_2 + (c_2 + c_{t2})\dot{z}_2 + (k_2 + k_{t2})z_2 - c_2\dot{z} - k_2z + c_2l_2\dot{\phi} + k_2l_2\phi = c_{t2}\dot{q}_2 + k_{t2}q_2 \end{cases} = 0 \quad (1)$$

In the research of the automobile's vibration, the automobile's vibration in the time region is mainly applied for assessing the automobile's comfort. However, based on ISO 2631-1:1997 [11], the automobile's vibration responses in the frequency region also greatly affected the ride comfort and structure in the automobile's systems. Therefore, in this study, the vibration characteristic of the automobile in the frequency region will be researched and evaluated under different operation conditions of the automobile.

2.2. Calculating the vibration equations of the automobile in the frequency range

To establish the automobile's vibration equations in the frequency region as well as evaluate the vibration characteristic of the car in the frequency region, based on the automobile's vibration equation in the time region in Equation (1), the Laplace transfer function [21] is then used to convert Equation (1) in the time region (t) to the image function (s) in the frequency region with the excitation frequency of ω . Herein, $\omega = 2\pi f$ and $s = d/dt$.

The theory of the Laplace transfer function is described by: If a vibration function of $n(t)$ operates and depends on the variable time of $t > 0$ in its operation range defined by $\{a \text{ and } b\}$, based on the method of the Laplace transfer function, the image function of $n(t)$ defined by $N(s)$ is expressed as follows:

$$N(s) = \int_b^a e^{-st}n(t)dt, s = i\omega \quad (2)$$

or

$$n(t) \rightarrow N(s) \quad (3)$$

Similarly, based on the theory of the Laplace transfer function, the derivative equations of the image function of $n(t)$, $\dot{n}(t)$, and $\ddot{n}(t)$ are also written by Dang [21]:

$$\begin{cases} n(t) \rightarrow N(s) \\ \dot{n}(t) \rightarrow sN(s) - N(0) \\ \ddot{n}(t) \rightarrow s^2N(s) - sN(0) - \dot{n}(0) \\ \dots \\ \ddot{\ddot{n}}^{(n)}(t) \rightarrow s^nN(s) - s^{n-1}N(s) - \dots - N(0) \end{cases} \quad (4)$$

From the dynamic model of the car in **Figure 1**, at the initial condition of the automobile moving when $t = 0$, the vibration responses of the automobiles and front/rear wheel axles are equal to zero ($z(t) = 0$, $\varphi(t) = 0$, $z_1(t) = 0$, and $z_2(t) = 0$). Therefore, the derivative equations of their image function at the initial condition when $t = 0$ are also equal to zero ($N(0) = 0$).

Based on the Laplace transfer function in Equations (3) and (4), the derivative equations of the automobile body's vertical vibration $z(t)$, automobile body's pitch vibration $\varphi(t)$, front axle's vibration $z_1(t)$, and rear axle's vibration $z_2(t)$ calculated in Equation (1) at the time region are described by the image functions (s) of $Z(s)$, $\Psi(s)$, $Z_1(s)$, and $Z_2(s)$ in the frequency region as follows:

$$\begin{cases} z(t) \rightarrow Z(s) \\ \dot{z}(t) \rightarrow sZ(s) \\ \ddot{z}(t) \rightarrow s^2Z(s) \end{cases}, \begin{cases} \varphi(t) \rightarrow \Psi(s) \\ \dot{\varphi}(t) \rightarrow s\Psi(s) \\ \ddot{\varphi}(t) \rightarrow s^2\Psi(s) \end{cases}, \begin{cases} z_{1,2}(t) \rightarrow Z_{1,2}(s) \\ \dot{z}_{1,2}(t) \rightarrow sZ_{1,2}(s) \\ \ddot{z}_{1,2}(t) \rightarrow s^2Z_{1,2}(s) \end{cases}, \text{ and } \begin{cases} q_{1,2}(t) \rightarrow Q_{1,2}(s) \\ \dot{q}_{1,2}(t) \rightarrow sQ_{1,2}(s) \end{cases} \quad (5)$$

Thus, the automobile's vibration equation of Equation (1) in the time region is rewritten by the automobile's vibration equation at the frequency range via the theory of Laplace functions as follows:

$$\begin{cases} a_{11}Z(s) + a_{12}\Psi(s) + a_{13}Z_1(s) + a_{14}Z_2(s) = 0 \\ a_{21}Z(s) + a_{22}\Psi(s) + a_{23}Z_1(s) + a_{24}Z_2(s) = 0 \\ a_{31}Z(s) + a_{32}\Psi(s) + a_{33}Z_1(s) + 0 = b_3Q_1(s) \\ a_{41}Z(s) + a_{42}\Psi(s) + 0 + a_{44}Z_2(s) = b_4Q_2(s) \end{cases} \quad (6)$$

By dividing Equation (6) by $Q_1(s)$, the matrix of Equation (6) has been rewritten by:

$$\begin{bmatrix} a_{11} & a_{12} & a_{13} & a_{14} \\ a_{21} & a_{22} & a_{23} & a_{24} \\ a_{31} & a_{32} & a_{33} & 0 \\ a_{41} & a_{42} & 0 & a_{44} \end{bmatrix} \begin{bmatrix} Z(s)/Q_1(s) \\ \Psi(s)/Q_1(s) \\ Z_1(s)/Q_1(s) \\ Z_2(s)/Q_1(s) \end{bmatrix} = \begin{bmatrix} 0 \\ 0 \\ b_3 \\ b_4Q_2(s)/Q_1(s) \end{bmatrix} \quad (7)$$

where $s = i\omega$, $s^2 = -\omega^2$, $a_{11} = -m\omega^2 + (k_1 + k_2) + i(c_1 + c_2)\omega$, $a_{12} = (k_1l_1 + k_2l_2) + i(c_1l_1 + c_2l_2)\omega$, $a_{31} = a_{13} = -k_1 - ic_1\omega$, $a_{41} = a_{14} = -k_2 - ic_2\omega$, $a_{21} = (k_1l_1 + k_2l_2) + i(c_1l_1 + c_2l_2)\omega$, $a_{22} = -I\omega^2 + (k_1l_1l_1 + k_2l_2l_2) + i(c_1l_1l_1 + c_2l_2l_2)\omega$, $a_{32} = a_{23} = -k_1l_1 - ic_1l_1\omega$, $a_{42} = a_{24} = -k_2l_2 - ic_2l_2\omega$, $a_{33} = -m_1\omega^2 + (k_1 + k_{t1}) + i(c_1 + c_{t1})\omega$, $a_{34} = -m_2\omega^2 + (k_2 + k_{t2}) + i(c_2 + c_{t2})\omega$, $b_3 = k_{t1} + ic_{t1}\omega$, and $b_4 = k_{t2} + ic_{t2}\omega$, respectively.

Let $T_z = Z(s)/Q_1(s)$, $T_\varphi = \Psi(s)/Q_1(s)$, $T_{z1} = Z_1(s)/Q_1(s)$, and $T_{z2} = Z_2(s)/Q_1(s)$, thus, T_z , T_φ , T_{z1} , and T_{z2} are defined as the vibration's transfer functions from the road to the automobile body and front/rear axles, respectively.

Based on the calculated results in the study of Dang [21], the result of the acceleration amplitude obtained via $T_n = \{T_z, T_\varphi, T_{z1}, \text{ and } T_{z2}\}$ in Equation (7) under road's excitations $Q_1(s)$ are written as follows:

$$|\ddot{T}_n| = \omega^2 \sqrt{X_n^2 + Y_n^2} = \omega^2 f_n(\omega) \quad (8)$$

2.3. Road's excitations on car's wheels

When the automobile is traveling on the road, the vibration excitation of the road described by the harmonic function with its wavelength from 5 m to 10 m and its

height from 0.01 m to 0.012 m greatly affects the automobile's ride comfort and structure [12,22,23]. This harmonic function mainly causes resonant vibrations in the automobile's suspension system. Thus, this excitation is used to evaluate the vibration characteristic of the automobile at the frequency range. The road surface's vibration equation using the harmonic surface at time region has been described as:

$$q_1 = q_0 \sin \omega t = q_0 \sin(2\pi/T)t \tag{9}$$

With the frequency and wavelength of the road defined by L and l , Equation (9) is then rewritten in the traveling direction of X as follows:

$$q_1 = q_0 \sin LX = q_0 \sin(2\pi/l)X \tag{10}$$

With an unchanged speed of the automobile (v), thus, $X = vt$. Both Equations (9) and (10) are then rewritten by:

$$q_1 = q_0 \sin \omega t = q_0 \sin(2\pi v/l)t \tag{11}$$

The basic length of the automobile is defined by $(l_1 + l_2)$, as shown in **Figure 1**, thus, the vibration excitation at the rear tire (q_2) calculated based on the vibration excitation at the front tire is expressed by:

$$q_2 = q_0 \sin \omega (t - t') = q_0 \sin \frac{2\pi v}{l_1 + l_2} (t - \frac{X}{v}) \tag{12}$$

From the ratio of q_2/q_1 calculated based on Equations (11) and (12), the Laplace transformation T_q of q_2/q_1 is then described by:

$$T_q = Q_2(s)/Q_1(s) = \cos[2\pi(l_1 + l_2)/l] - i \sin[2\pi(l_1 + l_2)/l] \tag{13}$$

Equation (13) is then used as the vibration excitation of the automobile to evaluate the characteristic of the automobile's vibrations in the frequency region.

3. Simulation and analysis result

Based on the automobile's excitations using the road's harmonic function with $q_0 = 10$ mm and the road's wavelength $l = 8$ m as well as the dynamic parameters of the automobile listed in **Table 1**, the vibration characteristic of the automobile in the frequency region under the different operation conditions is then simulated and analyzed.

Table 1. Automobile's dynamic parameters.

Parameters	Values	Parameters	Values	Parameters	Values
m (kg)	1384	k_1 (N/m)	90,880	c_1 (Ns/m)	7733
m_1 (kg)	66	k_2 (N/m)	93,884	c_2 (Ns/m)	9804
m_2 (kg)	87	k_{t1} (N/m)	193,211	c_{t1} (Ns/m)	2000
I (kg·m ²)	11,632	k_{t2} (N/m)	226,422	c_{t2} (Ns/m)	2000
l_1 (m)	1.35	l_2 (m)	1.604	q_0 (mm)	10

3.1. Automobile's vibration characteristic under different stiffness of the suspension system

To evaluate the effect of stiffness parameters in the automobile's systems on the characteristic of the acceleration-frequency in the automobile, three different stiffness parameters of the automobile's suspension system, including $K = [80\%, 100\%, 120\%] \times \{k_{1,2}, k_{t1,2}\}$ are simulated when the automobile is traveling on the road surface with

the harmonic function of $q_0 = 10$ mm and wavelength $l = 8$ m at $v = 20$ m/s. Results in the acceleration-frequency of the automobile's body in the vertical and pitching vibrations have been shown in **Figure 2a,b**.

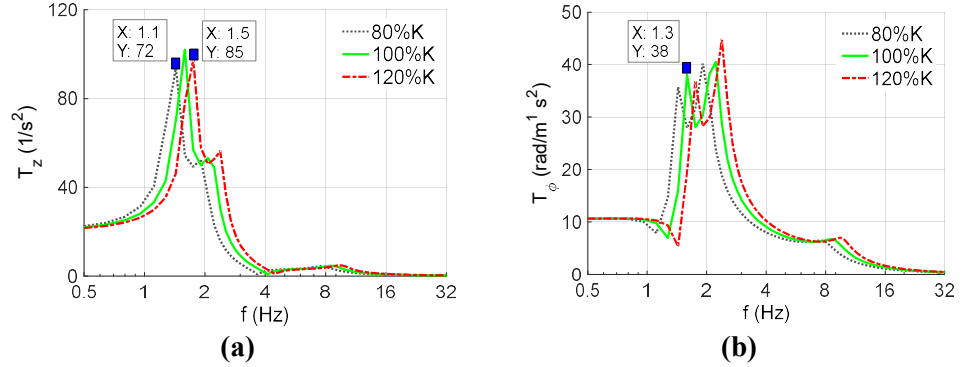


Figure 2. The response of the automobile body's acceleration-frequency under different stiffness values; **(a)** the vertical acceleration-frequency; **(b)** the pitching acceleration-frequency.

The simulation results show that both the responses of the acceleration frequency of the automobile's body in the vertical and pitching directions are significantly affected by the different stiffness coefficients of the automobile's suspensions and wheels. Resonant frequencies in the vertical and pitching directions of the automobile in the low frequency region appeared at 1.1 Hz, 1.3 Hz, and 1.5 Hz when the stiffness parameters were reduced by 80% K , used by 100% K , and increased by 120% K , respectively. Additionally, the acceleration-frequency amplitude in the vertical and pitching directions of the automobile at low frequencies is also dependent on stiffness coefficients in the automobile's suspension systems and wheels. The automobile's acceleration-frequency amplitudes are increased with the increase of the stiffness parameters and vice versa. These results mean that the K of the automobile's suspensions and wheels not only influences the amplitude but also influences the resonant frequency of the automobile's acceleration frequency in both the vertical and pitching directions. In order to ameliorate the automobile's comfort as well as ensure the durability of the automobile's structures, the designed parameters in the stiffness of the automobile's suspensions and tires need to be chosen to minimize the amplitude of the automobile's acceleration frequency at resonant frequencies.

3.2. Automobile's vibration characteristic under different mass

The analysis results in Section 3.1 show that the automobile's acceleration-frequency amplitudes and resonant frequencies are affected by the stiffness parameters of the automobile. Besides, based on the formula used to determine the resonant frequency of the system, the resonant frequency is calculated by $f^2 = K/M$. Thus, the automobile's mass (M) is also influenced by the automobile's acceleration-frequency characteristic. To clearly illustrate this issue, the automobile's different masses, including $M = [80\%, 100\%, 120\%] \times \{m, m_1, m_2\}$ are also simulated under the same excitation of the road surface in Section 3.1. The results of the acceleration-frequency of the automobile's body in the vertical and pitching vibrations are plotted in **Figure 3a,b**.

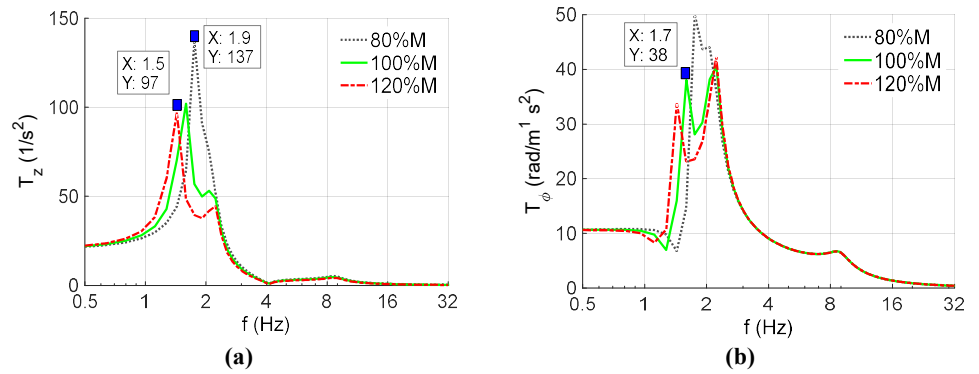


Figure 3. The response of the automobile body’s acceleration-frequency under different load conditions; **(a)** the vertical acceleration-frequency; **(b)** the pitching acceleration-frequency.

The simulation results indicate that both the responses of the acceleration-frequency of the automobile’s body in the vertical and pitching direction are also significantly affected by the different masses in the automobile’s body and front/rear axles. The resonant frequencies in the vertical and pitching directions of the automobile in the low frequency region appear at 1.5 Hz, 1.7 Hz, and 1.9 Hz when the automobile’s mass is increased by 120% M , used by 100% M , and reduced by 80% M , respectively. These resonant frequencies changed is due to the change of the automobile’s mass under the same stiffness parameters of the automobile suspension system ($f = \sqrt{k/m}$). Besides, the amplitude of the acceleration-frequency in the vertical and pitching direction of the automobile in the low frequency region is also dependent on the automobile’s mass. The automobile’s acceleration-frequency amplitudes are increased when the automobile’s mass is reduced and vice versa. This also means that the automobile’s mass not only influences amplitudes but also influences resonant-frequencies of the automobile’s acceleration frequency in both the vertical and pitching direction. The analysis results show that both the resonant frequencies and acceleration-frequency amplitudes of the automobile are mainly appeared in a low frequency region from 1.0 to 3.0 Hz under the effect of the automobile’s mass. This frequency region greatly affects the driver’s comfort and health, according to ISO 2631-1 [11]. In order to ameliorate automobile’s comfort and ensure durability in the automobile’s structures, in the design process of the automobile, both the mass M and stiffness K of the automobile’s systems should be calculated and chosen to minimize the amplitude of the acceleration-frequency at the resonant frequencies.

3.3. Automobile’s vibration characteristic under road’s different wavelengths

In the automobile’s condition traveling on the pavement, the road wavelength can affect the automobile’s ride comfort. To clear this issue, three different wavelengths of the road, including $l = 6$ m, $l = 8$ m, and $l = 10$ m, at the same excitations of the road in Section 3.1, are simulated, respectively. The results of the acceleration-frequency of the automobile’s body in the vertical and pitching vibrations are plotted in **Figure 4a,b**.

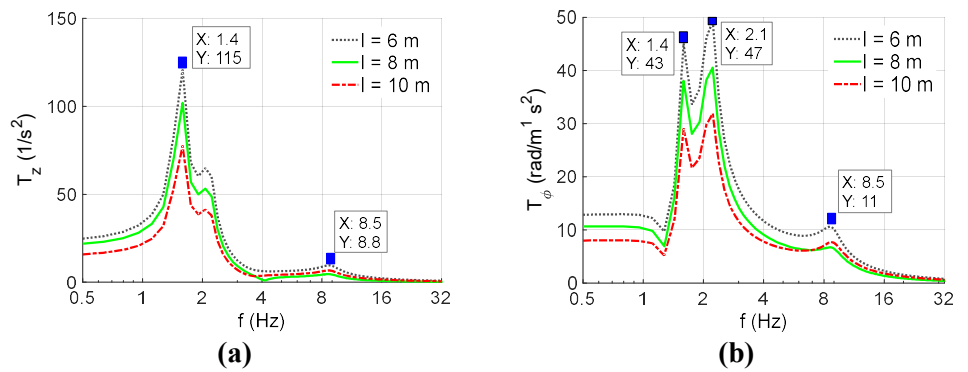


Figure 4. The response of the automobile body’s acceleration-frequency under road’s different wavelengths; **(a)** the vertical acceleration-frequency; **(b)** the pitching acceleration-frequency.

Under the effect of the different wavelengths of the road surface, the simulation results in **Figure 4a,b** show that the resonant frequencies of the automobile’s body in the vertical and pitching vibrations un-change and appear at 1.4 Hz, 2.1 Hz, and 8.5 Hz under the different values of the road wavelength. This means that the road wavelength does not influence the characteristics of the automobile’s acceleration frequency. However, the amplitude of the acceleration-frequency in the vertical and pitching direction of the automobile in the low-frequency region is changed and affected by the road’s different wavelengths. Their amplitude is increased when the road’s wavelength is reduced, and vice versa. This is because the excitation frequency of the road surface wave length with $l = 6$ m nearly coincides with the natural frequency of the automobile suspension system, thus the automobile’s acceleration frequency is increased. Thus, to reduce the amplitude of the acceleration-frequency in the vertical and pitching direction of the automobile, the road’s wavelength needs to be increased. This means that the pavement’s roughness needs to be decreased or the pavement’s surface quality needs to be enhanced. In addition, during the road design process, the road surface wave length needs to be considered, limiting the road surface wave length to less than 6 m to reduce the resonance vibrations of vehicles when moving on the road surface. This contributes to improving vehicle comfort and structural durability and reducing the potential risk of traffic accidents. This issue is also proven and recommended in existing studies [24].

4. Conclusions

This study uses the complex-domain method for evaluating automobile’s vibrations in the frequency region. The study can be summarized as follows:

The design parameters of stiffness, mass, and road wavelength remarkably affect the characteristics of the automobile’s acceleration frequency.

To reduce resonant amplitudes of the automobile’s acceleration frequency in both vertical and pitching directions, stiffness parameters in the automobile’s suspensions and tires should be reduced while the mass of the automobile’s body should be increased. However, the reduction of the stiffness of the automobile can lead to reduced stability and safety of movement of the automobile. To solve this issue, the automobile’s suspension systems are researched and replaced by using air suspension

systems or active suspension systems.

The resonant amplitude of the acceleration-frequency in the vertical and pitching direction of the automobile is significantly affected by the road wavelength; thus, to reduce this resonant amplitude, the pavement's roughness needs to be decreased or the pavement's surface quality needs to be enhanced.

From the main findings of this study, the analysis of automobile vibrations in the low frequency region has shed light on the influence of automobile dynamic parameters such as automobile mass, suspension stiffness, and road surface wave length on the ride comfort of the automobile and the structural durability of the suspension system through the automobile's frequency-amplitude response. Therefore, the study method of automobile vibrations using the Laplace transfer function can be applied to research all multi-axle heavy trucks, commercial vehicles, or vibrating rollers. This is the advantage of this study.

Author contributions: study conception and design, YJ and VN; design of the vehicle model, simulation, analysis results, YJ; writing, VN. All authors have read and agreed to the published version of the manuscript.

Conflict of interest: The authors declare no conflict of interest.

References

1. Yang Y, Ren W, Chen L, et al. Study on ride comfort of tractor with tandem suspension based on multi-body system dynamics. *Applied Mathematical Modelling*. 2009; 33(1): 11-33. doi: 10.1016/j.apm.2007.10.011
2. Nariman-Zadeh N, Salehpour M, Jamali A, et al. Pareto optimization of a five-degree of freedom vehicle vibration model using a multi-objective uniform-diversity genetic algorithm (MUGA). *Engineering Applications of Artificial Intelligence*. 2010; 23(4): 543-551. doi: 10.1016/j.engappai.2009.08.008
3. Pekgökgöz R, Gurel M, Bilgehan M, et al. Active suspension of cars using fuzzy logic controller optimized by genetic algorithm. *International of Journal Engineering Application Sciences*. 2010; 2(4): 27-37.
4. Ghoniem M, Awad T, Mokhiamar O. Control of a new low-cost semi-active vehicle suspension system using artificial neural networks. *Alexandria Engineering Journal*. 2020; 59(5): 4013-4025. doi: 10.1016/j.aej.2020.07.007
5. Zhu Y, Bian X, Su L, et al. Ride Comfort Improvement with Preview Control Semi-active Suspension System Based on Supervised Deep Learning. *SAE International Journal of Vehicle Dynamics, Stability, and NVH*. 2021; 5(1). doi: 10.4271/10-05-01-0003
6. Wang H, Kin Wong P, Zhao J, et al. Observer-based robust gain-scheduled control for semi-active air suspension systems subject to uncertainties and external disturbance. *Mechanical Systems and Signal Processing*. 2022; 173: 109045. doi: 10.1016/j.ymsp.2022.109045
7. Félix-Herrán LC, Mehdi D, Rodríguez-Ortiz J de J, et al. H_∞ control of a suspension with a magnetorheological damper. *International Journal of Control*. 2012; 85(8): 1026-1038. doi: 10.1080/00207179.2012.674216
8. Maciejewski I. Control system design of active seat suspensions. *Journal of Sound and Vibration*. 2012; 331(6): 1291-1309. doi: 10.1016/j.jsv.2011.11.010
9. Wang L, Li J, Yang Y, et al. Active control of low-frequency vibrations in ultra-precision machining with blended infinite and zero stiffness. *International Journal of Machine Tools and Manufacture*. 2019; 139: 64-74. doi: 10.1016/j.ijmachtools.2018.11.004
10. Zhu T, Wan H, Wang Z, et al. Model reference adaptive control of semi-active suspension model based on adaboost algorithm for rollover prediction. *SAE International Journal of Vehicle Dynamics, Stability, and NVH*. 2022; 6(1): 71-86. doi:10.4271/10-06-01-0005
11. ISO 2631-1:1997. Mechanical Vibration and Shock-Evaluation of Human Exposure to Whole Body Vibration-Part 2. International Organization for Standardization; 1997.
12. ISO 8068. Mechanical Vibration Road Surface Profiles Reporting of Measured Data. International Organization for

- Standardization; 1995.
13. Sun L. Optimum design of road-friendly vehicle suspension system subjected to rough pavement surfaces. *Applied Mathematical Modelling*. 2002; 25(5): 635-652. doi:10.1016/S0307-904X(01)00079-8
 14. Sun X, Zhang J. Performance of earth-moving machinery cab with hydraulic mounts in low frequency. *Journal of Vibration and Control*. 2014; 20(5): 724-735. doi:10.1177/10775463124642
 15. Ye S, Hou L, Zhang P, et al. Transfer path analysis and its application in low-frequency vibration reduction of steering wheel of a passenger vehicle. *Applied Acoustics*. 2020; 157: 107021. doi: 10.1016/j.apacoust.2019.107021
 16. de Brett M, Butlin T, Nielsen OM. Analysis of nonlinear vibration transmission through a vehicle suspension damper at low audio frequencies. *Journal of Sound and Vibration*. 2023; 551: 117615. doi: 10.1016/j.jsv.2023.117615
 17. Lakhdar Z, Chorfi SM, Belalia SA, et al. Free vibration and bending analysis of porous bi-directional FGM sandwich shell using a TSDT p-version finite element method. *Acta Mechanica*. 2024; 235: 3657-3686. doi: 10.1007/s00707-024-03909-y
 18. Belabed Z, Abdelouahed T, Mohammed A, et al. On the elastic stability and free vibration responses of functionally graded porous beams resting on Winkler-Pasternak foundations via finite element computation. *Geomechanics and Engineering*. 2024; 36(2): 183-204. doi:10.12989/gae.2024.36.2.183
 19. Bentrar H, Mohammed S, Belalia S, et al. Effect of porosity distribution on free vibration of functionally graded sandwich plate using the P-version of the finite element method. *Structural Engineering and Mechanics*. 2023; 88(6): 551-567. doi:10.12989/sem.2023.88.6.551
 20. Mesbah A, Belabed Z, Amara K, et al. Formulation and evaluation a finite element model for free vibration and buckling behaviours of functionally graded porous (FGP) beams. *Structural Engineering and Mechanics*. 2023; 86(3): 291-309. doi: 10.12989/sem.2023.86.3.291
 21. Dang V. Influence of Structural Parameters and Operating on Vietnam's Bus Ride Comfort. Hanoi University of Science and Technology, Vietnam; 1996.
 22. Nguyen SD, Nguyen QH, Choi SB. A hybrid clustering based fuzzy structure for vibration control – Part 2: An application to semi-active vehicle seat-suspension system. *Mechanical Systems and Signal Processing*. 2015; 56-57: 288-301. doi: 10.1016/j.ymsp.2014.10.019
 23. Zhu G, Du X, Liu W, et al. A novel method to solve the existed paradox of low-frequency vibration isolation and displacement attenuation in a nonlinear floating-slab on the wheel-rail loads. *Mechanical Systems and Signal Processing*. 2024; 208: 110985. doi: 10.1016/j.ymsp.2023.110985
 24. Yang J, Nguyen V, Wang X, et al. Performance study of semi-active seat suspension added by quasi-zero stiffness structure under various vibratory roller models. *Proc. IMechE, Part D: Journal of Automobile Engineering*. 2023; 237(6): 1-15. doi:10.1177/0954407022114316